DOI: https://doi.org/10.54966/jreen.v27i1.1157 - *Journal of Renewable Energies 27 (2024) 115 – 131*

Journal of Renewable Energies

Revue des Energies Renouvelables

journal home page: https://revue.cder.dz/index.php/rer

Research paper

Hydrogen fuel cell electric vehicles controlled by direct torque control (DTC) during low-speed operation

Farid Tazerart [a,*], Ahmed Azib [a], Farid Kerrouche [a], Toufik Rekioua [a]

[a] *Laboratoire de Technologie Industrielle et de l'Information (LTII), Faculté de Technologie, Université de Bejaia, 06000 Bejaia, Algérie.*

ARTICLE INFO

Article history:

Received January 16, 2024

Accepted June 29, 2024

Keywords:

Direct torque control,
Self-tuning fuzzy controller,
Fuel Cell,
Electric Vehicle.

ABSTRACT

Controlling the speed and torque of electric vehicles (EVs) under various road conditions poses a significant challenge with conventional control methods. This paper introduces a novel approach to direct torque control (DTC) by incorporating a self-tuning fuzzy speed controller specifically designed for EV applications. The self-tuning fuzzy proportional-integral-derivative (PID) controller is devised to continually update its output scaling factor. DTC, which directly links torque and speed control to the electromagnetic state of the motor, eliminates the need for a modulator. It performs effectively at high speeds and operates without a speed sensor. However, DTC is typically employed in the medium and low-speed range of electric vehicle propulsion. This paper aims to develop a DTC structure utilizing a self-tuning fuzzy speed controller for driving a fuel cell electric vehicle in low-speed urban scenarios. Simulation results demonstrate that the adaptive fuzzy PI control ensures better efficiency compared to the conventional PI controller, affirming its superior control performance.

1. INTRODUCTION

In recent times, there has been a notable shift towards the consideration of electric vehicles (EVs) as potential replacements for traditional automobiles. Since the 1970s, a growing emphasis has been placed on hybrid electric vehicles (HEVs), incorporating power components like engines, motors, and batteries. This integration enables them to leverage the strengths of both fully electric and conventional automobiles. Various configurations of electric and hybrid vehicles have been identified by researchers such as (Yue et al., 2023; Cao et al., 2023). These configurations include electric vehicles equipped with electric batteries and/or supercapacitors, hybrid electric vehicles that combine traditional propulsion

* *Corresponding author, E-mail address: farid.tazerart@univ-bejaia.dz*
Tel : + 213 75560587

ISSN: 1112-2242 / EISSN: 2716-8247

with electric motors powered by batteries or supercapacitors, and electric vehicles equipped with fuel cell batteries as proposed by (De Wolf et al., 2023).

Presently, electric vehicles stand as a practical alternative to traditional automobiles, offering the advantages of zero gas emissions, particle emissions, and quiet operation. Recognized as an impactful and viable solution, electric vehicles play a role in alleviating the environmental consequences associated with transportation.

In contrast to a conventional internal combustion engine car, which can travel between 550 to 1,000 kilometers on a full tank of gasoline or diesel, electric cars typically have an average range of 200 to 490 kilometers. Notably, hydrogen fuel cell electric vehicles of the latest generation surpass many other types of electrified vehicles in terms of distance coverage, providing a range exceeding 400 kilometers.

Electric vehicles featuring fuel cell batteries and hybrid vehicles have garnered significant attention in the industrial sector and are swiftly emerging as solutions to energy and ecological challenges. Fuel cell electric vehicles (FCEVs) utilize a fuel cell battery powered by hydrogen to generate electricity for an electric motor. FCEVs employ the battery for activities such as recapturing braking energy, providing additional power during short acceleration events, and smoothing out the power delivery from the fuel cell. This includes the option to idle or turn off the fuel cell during periods of low power demand. Leveraging efficient electric motors, electric vehicles offer a means to establish a clean and efficient urban transport system, fostering a more environmentally friendly environment (Armenta-Déu et al., 2023; Bayindir et al., 2011).

Various control techniques employing power electronics devices have evolved to enhance the performance of electric motors (Jia-Sheng et al., 2011). Direct Torque Control (DTC) is a method utilized for regulating electric motors, selecting an appropriate voltage vector to control torque and flow. DTC boasts several advantages, including reduced dependence on machine parameters, simpler implementation, and quicker torque response (Tazerart et al., 2015). However, DTC is not without its drawbacks, including challenges in controlling torque and flux at very low speeds, high current ripple causing torque fluctuations, and variable switching frequency behavior (Abdelli et al., 2011).

When employing DTC control for electric vehicles, speed variables require regulation with a proportional-integral-derivative (PID) type controller. The main challenges in implementing a conventional PID algorithm for speed control in DTC lie in the effects of Ohmic voltage drop. The estimation of flux is typically calculated by integrating the voltage supplied to the motor, but due to errors in voltage measurement, knowledge of stator resistance, and the influence of Ohmic voltage drop, this integral becomes prone to inaccuracies at low speeds. Tuning the PID controller response is essential for achieving better oscillations, steady-state response, and reduced error by adjusting the PID parameters.

Fuzzy logic controllers (FLC) show promising results in the context of DTC when PID parameters are controlled using fuzzy rules. Various adaptive FLC types, including self-tuning and self-organizing controllers, have been developed and implemented for diverse practical processes.

The initial section of this paper delineates the concept of direct torque control. The subsequent segment outlines the framework of the self-tuning fuzzy logic controller of the proportional-integral (PI) type. Moving on to the third section, the paper introduces a PID parameters self-tuning fuzzy controller designed for the DTC control loop applied to the traction system of a hybrid electric vehicle equipped with a fuel cell battery. This involves adjusting the rules and membership functions of the controller. The final section presents simulation results, demonstrating the effective control performance. Moreover, the PID parameters self-tuning fuzzy controller exhibits robust and reliable performance across various systems.

2. STRATEGY FOR DIRECT TORQUE CONTROL

The DTC method utilizes a simple switching table to identify the optimal inverter state for attaining a desired output torque (El Ouanjli et al., 2019; Jasthi et al., 2023; Bensalah et al., 2023). It relies on flux and torque hysteresis controllers to determine the necessary voltage for driving the flux and torque to the target values. The algorithm for DTC is illustrated in Figure 1.

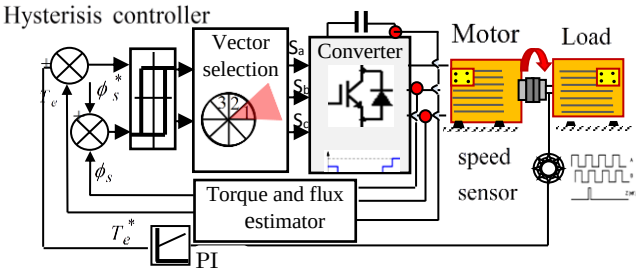

Fig 1. Simplified basic scheme of theDTC technique

2.1 Fundamental Direct Torque Control for Induction Motor

Starting with the machine model described in a reference frame tied to the stator, the estimation of the stator flux vector is derived from the following relationship:

$$\vec{\phi}_s(t) = \int_0^t (\vec{V}_s(t) - R_s \vec{i}_s(t))dt \tag{1}$$

The stator flux components $\phi_{s\alpha}$ and $\phi_{s\beta}$ can be estimated by:

$$\begin{cases} \phi_{s\alpha}(t) = \int (V_{s\alpha}(t) - R_s.i_{s\alpha}(t))dt \\ \phi_{s\beta}(t) = \int (V_{s\beta}(t) - R_s.i_{s\beta}(t))dt \end{cases} \tag{2}$$

Where: $V_{s\alpha}$, $V_{s\beta}$, $i_{s\alpha}$ and $i_{s\beta}$ are stator voltages and currents along α and β stator axes respectively.

The magnitude of the stator flux can then be estimated by:

$$\phi_s = \sqrt{{\phi_{s\alpha}}^2 + {\phi_{s\beta}}^2} \tag{3}$$

The phase angle of the stator flux can be calculated by:

$$\theta_s = \tan^{-1} \frac{\phi_{s\beta}}{\phi_{s\alpha}} \tag{4}$$

And the electromagnetic torque can be estimated by:

$$T_e = \frac{3}{2}.p.(\phi_{s\alpha} i_{s\beta} - \phi_{s\beta} i_{s\alpha}) \tag{5}$$

The complete block diagram of the induction motor (IM) drive system under DTC is depicted in Figure 1. The Proportional-Integral (PI) controller is employed to convert the speed feedback into the torque reference value, enabling the system to execute speed control. Consequently, both torque and speed can be regulated in this process.

2.2 Stator flux control

Figure.2 shows the voltage vectors which are usually used in DTC scheme with, as example, the stator flux located in sector 1.

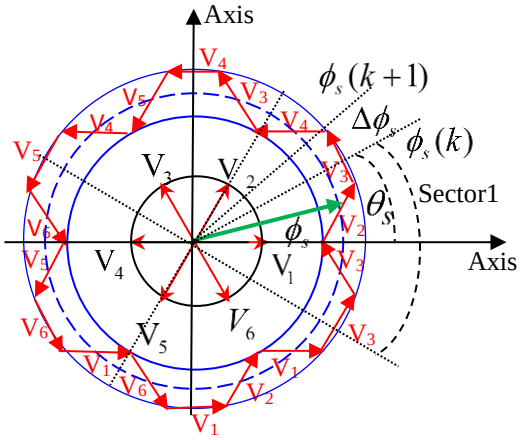

Fig 2. Stator flux trajectory with voltage vector selection

2.3 Switching Table for Flux and Torque Control

Based on the signals produced by the hysteresis controllers for stator flux and electromagnetic torque, a single voltage vector is chosen to manipulate torque and flux. The selection of this vector is contingent upon the outputs of the torque and flux controllers and the position of the stator flux vector, as illustrated in Table 1 (Bensalah et al., 2023).

Table 1. Switching table

H_ϕ	H_{Te}	S(1)	S(2)	S(3)	S(4)	S(5)	S(6)
	1	V_2	V_3	V_4	V_5	V_6	V_1
1	0	V_0	V_7	V_0	V_7	V_0	V_7
	-1	V_6	V_1	V_2	V_3	V_4	V_5
	1	V_3	V_4	V_5	V_6	V_1	V_2
-1	0	V_7	V_0	V_7	V_0	V_7	V_0
	-1	V_5	V_6	V_1	V_2	V_3	V_4

3. STRUCTURE OF THE FUZZY CONTROL REGULATOR

Fuzzy control is fundamentally an adaptive and nonlinear control method, known for its robust performance in the face of parameter variations in linear or nonlinear plants (Burkan et al., 2022). Departing from traditional quantitative techniques of system analysis and control, this approach employs linguistic variables in lieu of numerical variables. The fundamental configuration of a Fuzzy Logic Controller (FLC) featuring five linguistic variables (two inputs and three outputs) is depicted in Figure 3. The fuzzy controller is a system with two inputs (error and change in error) and three outputs (KP, KI, and KD). The error and the change in error are modeled using equations (6) and (7).

$$e(k) = \omega_{ref} - \omega_r \tag{6}$$

$$\Delta e(k) = e(k) - e(k-1) \tag{7}$$

where ω_{ref} is the reference speed, ω_r is the actual rotor speed, e(k) , Δe(k) represents the error, and the change in error. In Figure 3, the values of the parameters *Kp*, *Ki*, and *Kd* are adjusted using signals

derived from the fuzzy logic block, based on the variations in error between reference signals and output signals. In this context, $r(t)$ denotes the control signal, $y(t)$ is the output response, $e(t)$ is the error, and (De) is the derivative of the error.

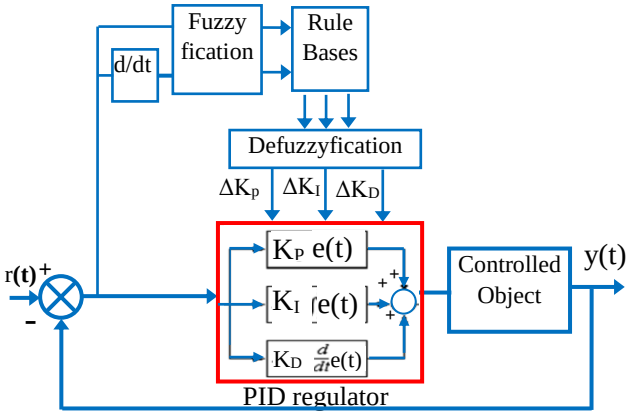

Fig 3. Basic block diagram of a fuzzy controller

4. PROPOSED DTC WITH SELF-TUNING FUZZY SPEED CONTROLLER

A simplified block diagram illustrating the (DTC) strategy with a speed control loop (Benbouhenni et al., 2019; Boukhalfa et al., 2022; Berabez et al., 2023) utilizing a self-tuned Fuzzy PID controller for an electric vehicle is depicted in Figure 4. In this system, the output of the "fuzzy logic controller" determines the torque, serving as the reference input for the DTC drive. Electric traction motor draws power from both the fuel cell and the traction battery pack, propelling the vehicle.

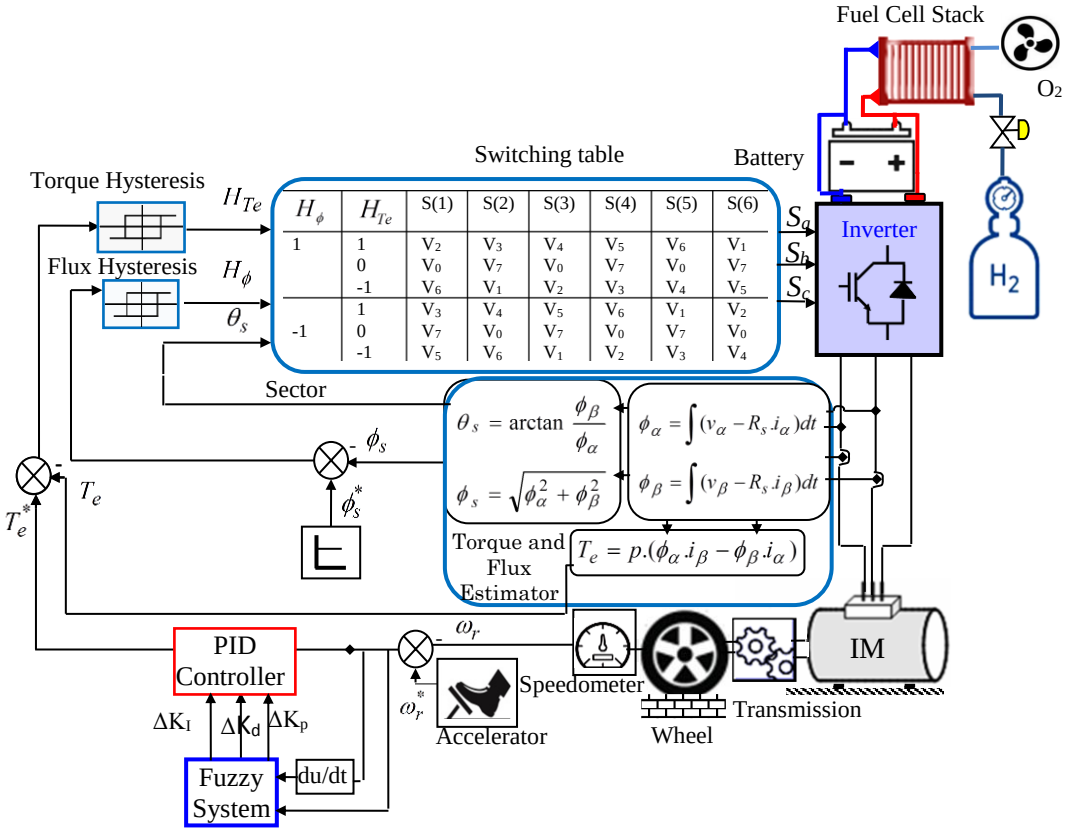

Fig 4. Illustrates the implementation of (DTC) with a speed control loop using a self-tuning Fuzzy PID controller for an electric vehicle

4.1 Self-Tuned Fuzzy PID for DTC

The term "self-tuning fuzzy PID controller" implies that the three parameters Kp, Ki, and Kd of the PID controller are adjusted using a fuzzy tuner (Tazerart et al., 2014; Bouguerra et al., 2023; Sayeh et al., 2024). The proportional, integral, and derivative terms are combined to compute the output of the PID controller. Therefore, automatic tuning of the PID parameters is essential. The configuration of the self-tuning fuzzy PID controller is depicted in Figure 5.

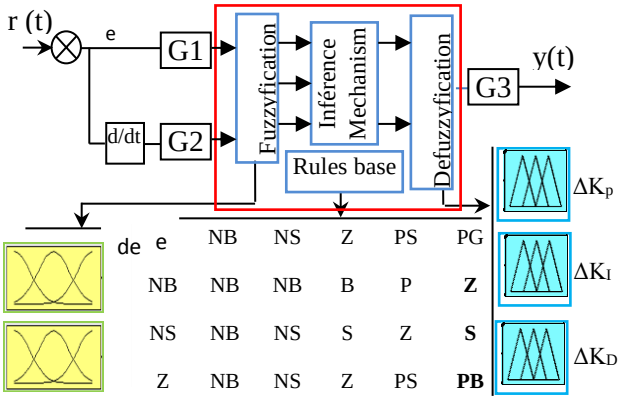

Fig 5. Structure of fuzzy self-tuning PID controller

The fuzzy self-tuning of PID parameters involves establishing a fuzzy relationship between the three PID parameters and the error ("e") and its derivative ("de"). Following the principles of fuzzy control, these three parameters are then adjusted to fulfill varied control parameter requirements when "e" and "de" exhibit variations. This process aims to ensure the control object exhibits satisfactory dynamic and static performance. The significance of the linguistic variables employed in the computation of Kp and KI regulators is elucidated in Table 2 and Table 3.

Table 2. Fuzzy rules for computation of Kp

Kp	*De*			
		NB	*Z*	*PB*
	NB	*Z*	*PB*	*Z*
e	*Z*	*Z*	*PS*	*PM*
	PB	*Z*	*PB*	*Z*

Table 3. Fuzzy rules for computation of K_I

Ki	*De*			
		NB	*Z*	*PB*
	NB	*P*	*Z*	*P*
e	*Z*	*P*	*P*	*P*
	PB	*P*	*Z*	*P*

5. ARCHITECTURE OF FUEL CELL ELECTRIC VEHICLE

The electric traction system, as depicted in Figure 6 (Visioli A, 2001; Zidane et al., 2024), is composed of four main components: Control strategy, DC/DC converter (Djermouni et al., 2024; Xingzhi , 2017; Mihăescu et al., 2018), inverter, and induction motor. In this configuration, the electric motor's power propels the drive train through mechanical transmission (Baodong, 2017; Li J et al., 2014). The fuel tank stores hydrogen gas on board the vehicle until it is needed by the fuel cell.

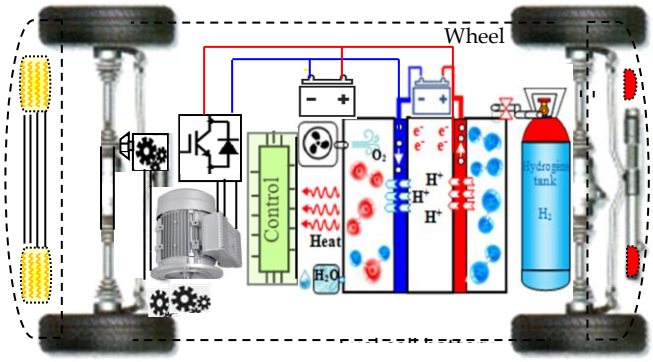

Fig 6. Electric drive powered by the fuel cell battery

The energy sources are dimensioned at maximum speed and maximum weight of the vehicle (the maximum speed is 80 Km/h and the maximum weight of the vehicle is 1540Kg). The motor used for the traction system is an induction motor (IM) of 37 kW. Then, the dimensions and characteristics of each element of the EV (batteries, voltage converters, traction and control systems) were selected according to the characteristics of the IM.

5.1 Vehicle dynamics model

This study formulates the electrical model for a fuel cell-based electric light vehicle, encompassing factors such as vehicle mass, wheel radius and mass, the vehicle's aerodynamic profile, and the motor drive, among other components. Figure 7 illustrates the forces that the electric machine of the vehicle must overcome.

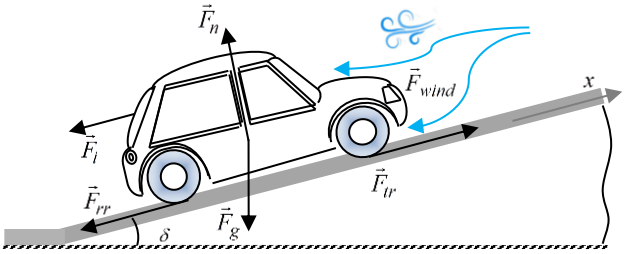

Fig 7. Forces acting vehicle moving along a slope

In this context, $\vec{F}_{tr}$ represents the traction force, $\vec{F}_i$ is the inertial force, $\vec{F}_{rr}$ denotes the rolling resistance force of the wheels, $\vec{F}_g$ stands for gravitational force, $\vec{F}_n$ i is the normal force, $\vec{F}_{wind}$ represents the force due to wind resistance, and δ is the angle of the driving surface. The traction force of a vehicle can be expressed as described by (Zhang, 2014; Liu Y et al., 2017):

$$\vec{F}_{tr} = \vec{F}_i + \vec{F}_{gx} + \vec{F}_{rr} + \vec{F}_{wind} \tag{8}$$

The power required to drive the EV at a speed v has to compensate the road load F_{tr} is given by:

$$P_{drive} = v.F_{tr} \tag{9}$$

Applying the principles of vehicle mechanics and aerodynamics, we can assess the power transmission and energy needed to sustain the vehicle's operation (refer to Figure 8).

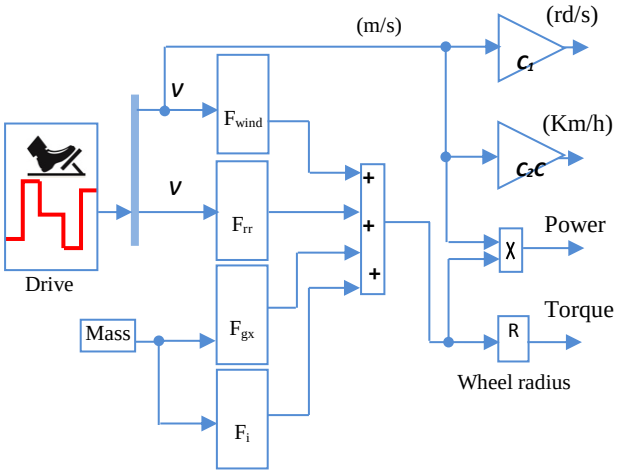

Fig 8. Functional diagram of theEV dynamics

5.2 Fuel cell battery

Illustrated in Figure 9, a fuel cell battery is an electrochemical device that merges hydrogen fuel with oxygen to generate electricity, heat, and water. Similar to a conventional battery, a fuel cell operates through an electrochemical reaction as long as fuel is supplied. Hydrogen is stored in a pressurized container, and oxygen is drawn from the air. Due to the absence of combustion, there are no harmful emissions, and the sole by-product is pure water.

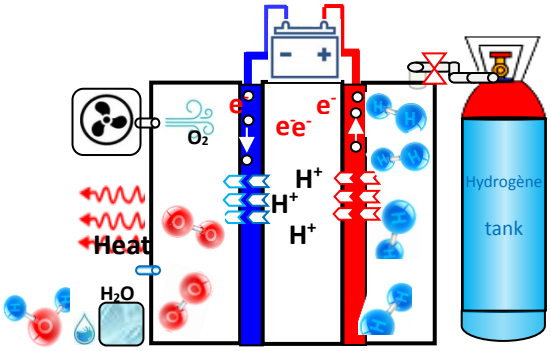

Fig 9. Principleof the fuel cell battery

The chemical reactions for the fuel cell battery system can be expressed as follows:

Anode reaction:

$$H_2(g) \rightarrow 2H^+ + 2e^- \tag{10}$$

Cathode reaction:

$$\frac{1}{2}O_2 + 2.H^+ + 2e^- \rightarrow H_2O(l) \tag{11}$$

Net:

$$H_2(g) + \frac{1}{2}O_2(g) \rightarrow H_2O(l) \tag{12}$$

The total output voltage V_{cell} of a single-cell can be calculated by the equation (13) as:

$$V_{cell} = E_{cell} - V_{ohmic} - V_{act} \tag{13}$$

Where E_{cell} is the single fuel cell thermodynamic voltage (V), V_{ohmic} is the ohmic voltage drop (V), V_{act} is the cell activation voltage drop (V).

The maximum power can be estimated by using the following equation (14) as:

$$P_{\max} = [\frac{1}{2}.\rho_{air}.V_t^2.S_{cx} + m..g.C_r + m\frac{dv}{dt}].V_t \tag{14}$$

Using equation (13), the maximum power is estimated at 30 kW.

5.3 Fuel cell battery model

The simulink and functional diagram of the subsystem block for the fuel cell battery is illustrated in Figure 10.

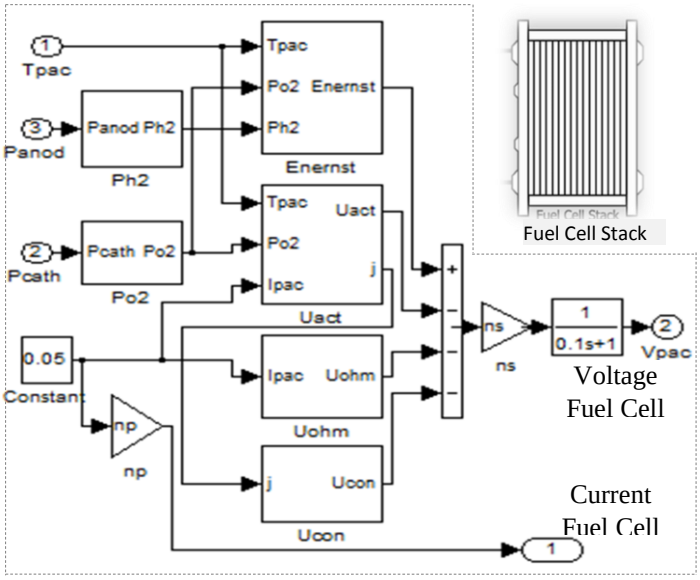

Fig 10. Functional diagram of the fuel cell battery

The energy sources are sized based on the maximum speed and weight of the vehicle (with a maximum speed of 80 km/h and a maximum weight of 1540 kg). The traction system employs a 37.kW induction motor (IM). Subsequently, the dimensions and specifications of each element in the electric vehicle (batteries, voltage converters, traction, and control systems) are chosen in alignment with the characteristics of the IM.

5.4 Converter model

The power electronics controller unit regulates the flow of electrical energy from both the fuel cell and the traction battery, governing the speed and torque output of the electric traction motor. The fuel cell battery is required to provide a continuous bus voltage (V_{DC}=400V) through the boost chopper, as depicted in Figure 11.

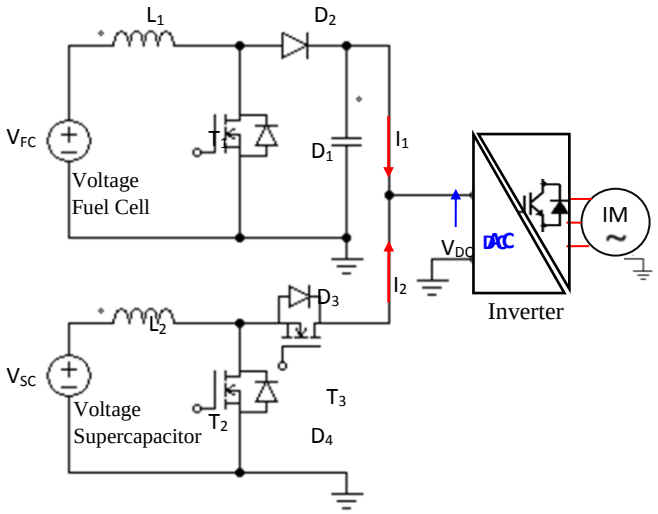

Fig 11. Boost chopper architecture

6. SIMULATION RESULTS

The dynamic and equilibrium states of the induction motor (IM), with parameters detailed in Table 4, powered by an inverter and controlled through direct torque control, were simulated utilizing MATLAB/Simulink software. The mechanical and aerodynamic characteristics of the electric vehicle are also provided in Table 5. The outcomes of the simulation are presented in Figures 12 to 24.

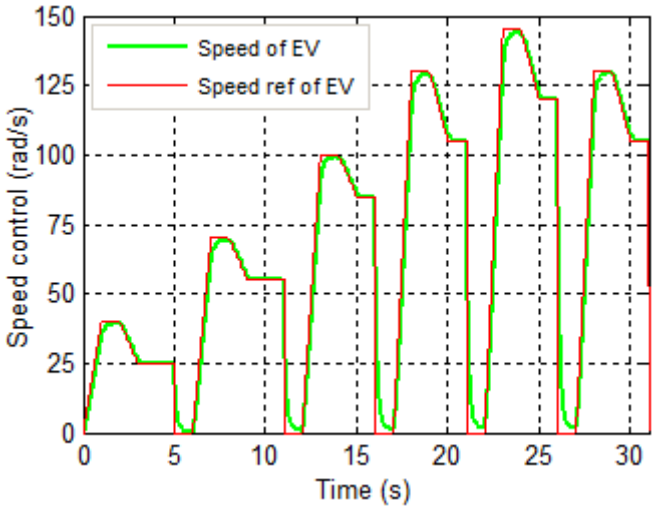

Fig 12. Vehicle wheels speed with test urban cycle

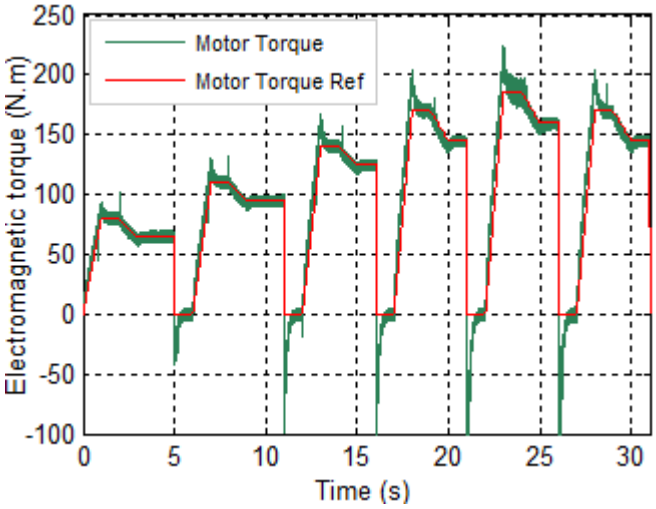

Fig 13. Motor torque

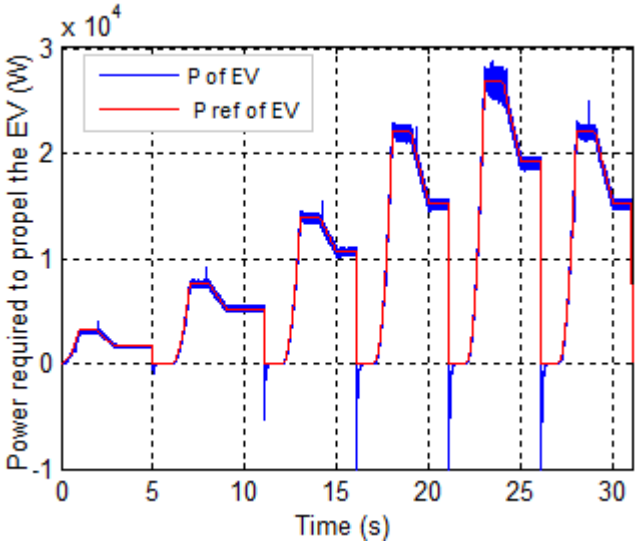

Fig 14. Power required to propel the EV

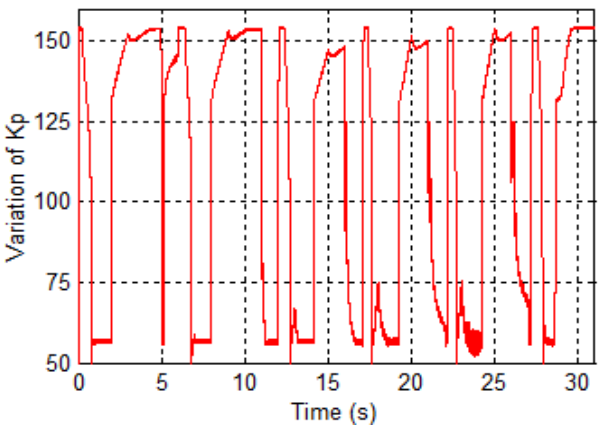

Fig 15. Kp with self-adaptive

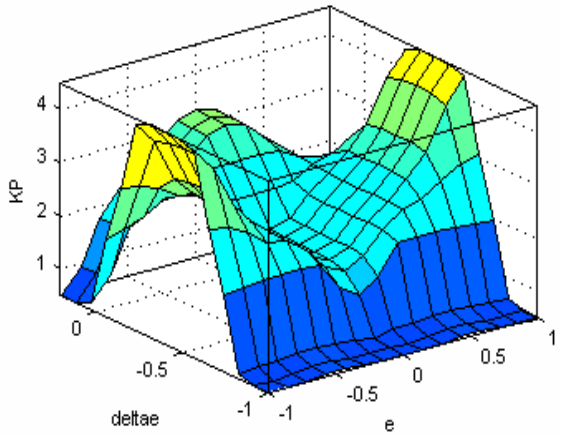

Fig 16. Surface view of fuzzy controller output for K_P

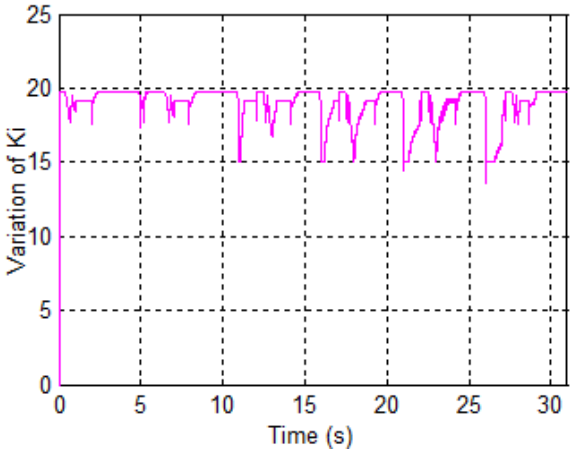

Fig 17. Ki with self-adaptive

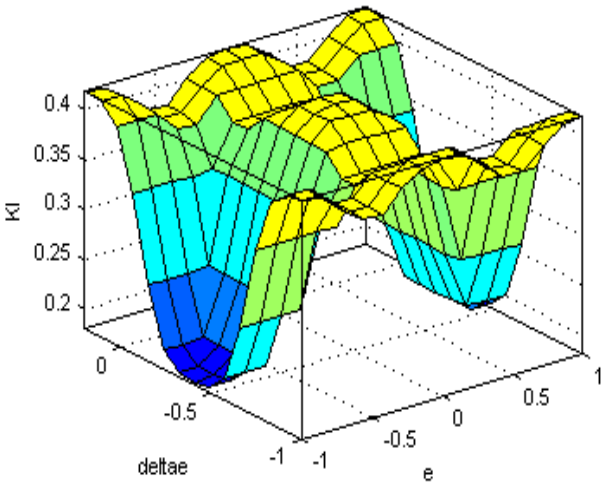

Fig 18. Surface view of fuzzy controller output for K_I

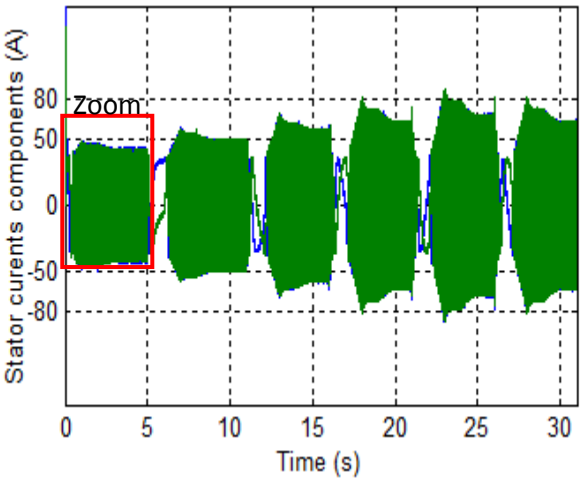

Fig 19. Instantaneous stator currents.

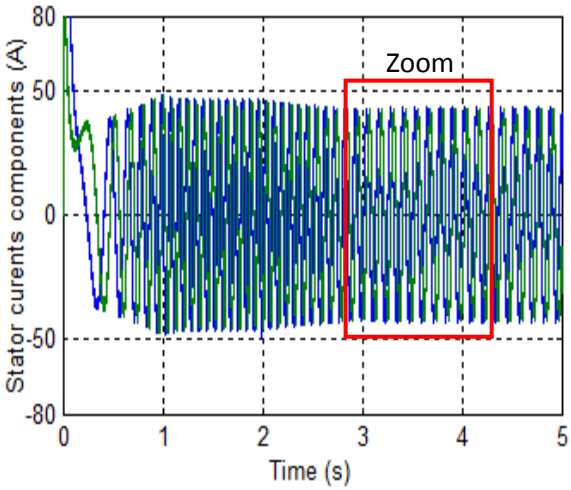

Fig 20. Zoom for stator currents at 0s to 5s

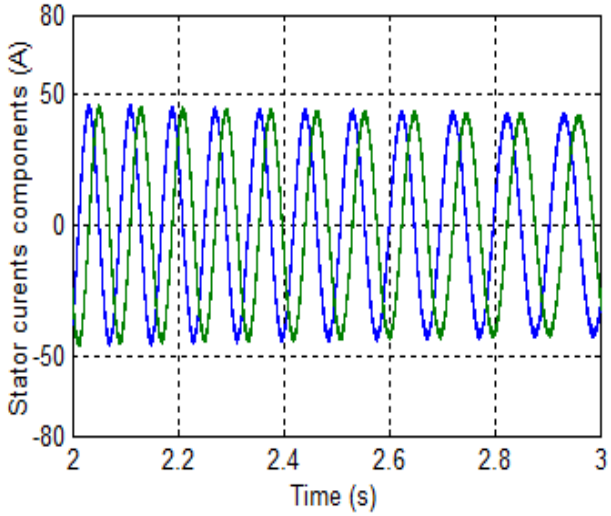

Fig 21. Zoom for stator currents at 2s to 3s

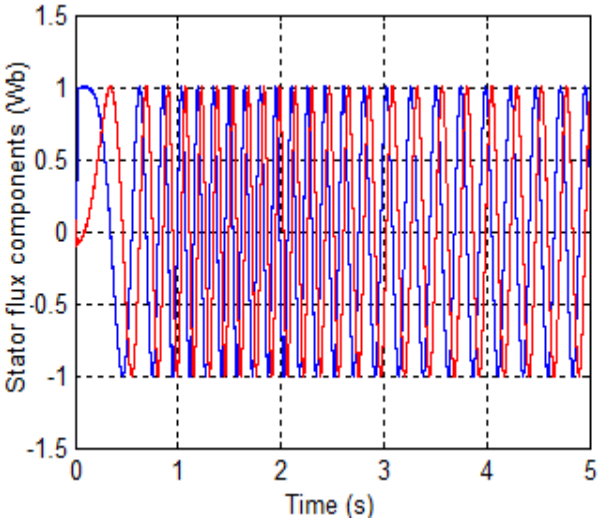

Fig 22. Stator flux components

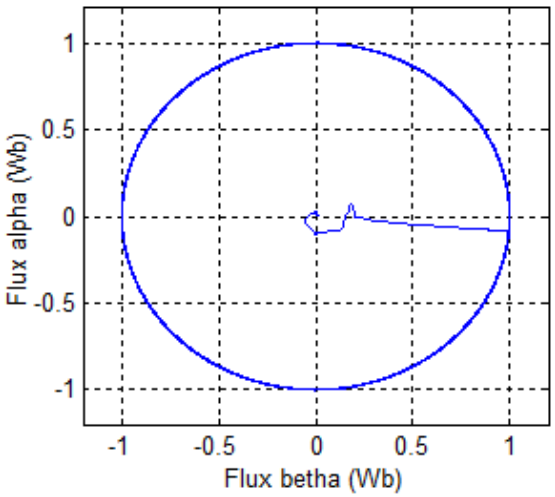

Fig 23. Circular trajectory of stator flux

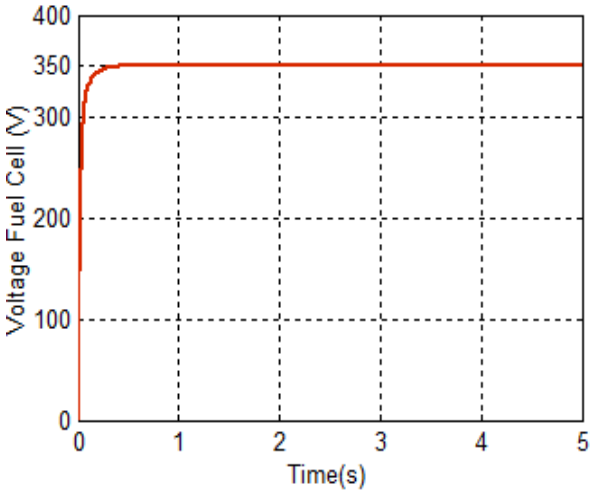

Fig 24. Voltage of the fuel cell battery

7. DISCUSSION OF RESULTS

In Figure 12, the test cycle and urban sequence depict a series of data points representing vehicle speed versus time, particularly characterized by low speeds (up to a maximum of 80 km/h). This cycle is valuable for assessing electric vehicle (EV) performance in urban environments. Figure 13 illustrates the dynamics of the EV, showcasing the developed torque in the induction motor alongside changes in acceleration, where the electromagnetic torque compensates for resisting torque. These figures demonstrate that the torque and speed reach their reference values, highlighting that the system, utilizing the Fuzzy self-adaptation speed regulator, enhances the precision of speed and torque control. Figure 14 depicts the power required to propel the EV. To determine the power drawn from the battery for tractive effort, various efficiencies at all operating points need to be considered. Figures 15 and 17 detail the variations of *KP* and *KI* respectively, concerning error (e) and the change in error (Δe). Figures 19, 20, and 21 showcase the robustness of stator currents, indicating that the stator current absorbed by the induction machine is nearly sinusoidal. Figures 22 and 23 exhibit steady stator flux waveforms, indicating that the proposed fuzzy control strategy not only enhances the precision of speed control and flux observation but also reinforces the robustness of the system.
The objective of voltage regulation is to maintain the output voltage of the DC bus at a constant value of 350V, irrespective of load variations.

8. CONCLUSION

To achieve high-performance control of an induction motor, this paper introduces a combined controller that integrates both Direct Torque Control (DTC) and artificial intelligence techniques. Specifically, the study focuses on implementing direct torque control of an induction machine utilizing a self-tuning speed controller. This is accomplished by integrating a self-adjusting regulator block into a traditional direct torque control system. The fuzzy regulator, known for its compelling dynamic performance, is employed as an alternative to the conventional PI-regulator. Notably, the synthesis of the fuzzy regulator is conducted without considering the machine model. Both simulations and theoretical results underscore the effectiveness of the proposed approach, combining DTC with a self-tuning speed controller.

This article contributes theoretical insights into low-speed Direct Torque Control (DTC), specifically designed for controlling an urban fuel-efficient vehicle. Here are some of the main results: The paper introduces a simple yet robust self-tuning mechanism for the direct torque control of an induction motor, specifically tailored for the low-speed traction of an urban fuel cell vehicle. This is achieved by integrating a self-adjusting regulator block into a traditional direct torque control system. The self-tuning fuzzy controller is employed to adjust the values of Kp and Ki for the proportional-integral (PI) controller.

Comparatively, the fuzzy regulator exhibits highly favorable dynamic performance when contrasted with the conventional PI-regulator. Notably, the synthesis of the fuzzy regulator is conducted without considering the machine model. Simulation results underscore the effectiveness of the proposed method, showcasing the efficacy of DTC with a self-tuning speed controller. The outcomes affirm that the designed self-tuned PID controller achieves commendable dynamic behavior in DTC, ensuring precise low-speed tracking with minimal overshoot, and it outperforms the conventional PID controller.

In conclusion, the proposed approach proves to be highly suitable for electric vehicle (EV) applications, particularly in the context of urban fuel cell vehicles operating at low speeds.

ACKNOWLEDGEMENTS

I wish to extend my heartfelt appreciation to the LTII laboratory and BEJAIA University for their invaluable support and contributions during the research and writing of this paper.

APPENDIX

Table 4. Parameters of the induction machine

Parameter	Value
Rated power	37 kW
Speed	1420 rpm
Voltage	230V
Stator current	I_s= 64 A
Stator resistance	R_s= 0.0851 Ω
Rotor resistance	R_r = 0.0658 Ω
Stator inductance	L_s= 0.0314 H
Rotor inductance	L_r= 0.0291 H
Mutual inductance	M= 0.0291 H
Number of pole pairs	P= 2

Table 5. Parameters of the EV and the traction system

Parameter	Value
Vehicle Mass	1540 Kg
Vehicle frontal area	1.8 m^2
Tire rolling resistance coeffi	0.015
Aerodynamic drag coefficient	0.25
Stokes coefficient	0.22
Air density	0.23 Kg/m^2
Wheel radius.	0.3 m
Transmission ratio.	2

NOMENCLATURE

C_1	Constant1	$i_{s\beta}$	Componentstator current along β axis, A
C_2	Constant2	R_s	Stator resistance, Ω
e	Error	L	Inductance, mH
Δe	Change of error	T_e	Electromagnetic torque, Nm
K_p	Proportional sensitivity	p	Pair-pole number of the induction machine
K_I	Integral sensitivity	g	Gravitational acceleration constant
V_s	Stator voltage vector	R	Wheel radius
$V_{s\alpha}$	Componentstator voltage along α axis,V	P_{drive}	Vehicle driving power, W
$V_{s\beta}$	Componentstator voltage along β axis,V	Out	Output
$i_{s\alpha}$	Componentstator current along α axis, A	Inp	Input

Greek symbols

α	Nomination for axis	v	Vehicle speed
β	Nomination for axis	δ	Grade angle
ϕ	Stator flux, Wb	ρ_{air}	Air density
θ_s	Angular position of flux, deg	ω_r	Rotor mechanical speed, rad/s
ω_{ref}	Reference rotor mechanical speed, rad/s		

Abbreviations

AC	Alternating Current	NS	Negative small
DC	Direct Current	PB	Positive big
D	Diode	PI	Proportional Integral controller
DTC	Direct Torque Control	PD	proportional derivative controller
EV	Electric Vehicle	PID	Proportional-Integral-Derivative controller
FC	Fuel Cell	PS	Positive small
FLC	Fuzzy Logic Controller	REF	Reference
IM	Induction Motors	T	Transistor
NB	Negative big	Z	Zero

REFERENCES

Abdelli, R., Rekioua, D., & Rekioua, T. (2011). Performances improvements and torque ripple minimization for VSI fed induction machine with DTC. *ISA Transactions*, *50*(2), 213-219. DOI:10.1016/j.isatra.2010.11.008

Armenta-Déu, C., & Arenas, A. (2023). Performance Analysis of Electric Vehicles with a Fuel Cell–Supercapacitor Hybrid System. *Engineering*, *4*(3), 2274-2292. DOI:10.3390/eng4030130

Bayindir, K. C., Gozukucuk, M. A., & Teke, A. (2011). A comprehensive overview of hybrid electric vehicle: Powertrain configurations, powertrain control techniques and electronic control units. *Energy Conversion and Management, 52*(2), 1305-1313. DOI: 10.1016/j.enconman.2010.09.028

Benbouhenni, H. (2019). Correcteur du couple à cinq niveaux pour la commande DTC douze secteurs basés sur la logique floue et les réseaux de neurones de la MAS de forte puissance. *Journal of Renewable Energies*, *22*(1), 113-121. DOI:10.54966/jreen.v22i1.731

Bensalah, M., & Harzallah, A. (2023). Modern Improvement Techniques of Direct Torque Control for Induction Motor Drives: A Review. *Protection and Control of Modern Power Systems, 8*, 52. DOI:10.1186/s41601-023-00276-2

Berabez, K., Hamoudi, F., Idjdarene, K., & Hacini, I. (2023). Fuzzy Logic PI controller based Direct Torque control of a Self-Excited Induction Generator through a three-level Rectifier. *Journal of Renewable Energies, ICARES 2022 (Special Issue)*, 1-12. DOI:10.54966/jreen.v1i1.1093

Bouguerra, Z. (2023). Comparative study between PI, FLC, SMC and Fuzzy sliding mode controllers of DFIG wind turbine. *Journal of Renewable Energies, 26*(2), 209-223. DOI:10.54966/jreen.v26i2.1146

Boukhalfa, G., Belkacem, S., Chikhi, A., & Benaggoune, S. (2022). Direct torque control of dual star induction motor using a fuzzy-PSO hybrid approach. *Applied Computing and Informatics*, *18*(1/2), 74-89. DOI:10.1016/j.aci.2018.09.001

Burkan, R., & Mutlu, A. (2022). Robust control of robot manipulators with an adaptive fuzzy unmodelled parameter estimation law. *Robotica, 40*(7), 2365-2380. DOI:10.1017/S0263574721001685

Cao, Y., Yao, M., & Sun, X. (2023). An Overview of Modelling and Energy Management Strategies for Hybrid Electric Vehicles. *Applied Sciences, 13*(10), 5947. DOI:10.3390/app13105947

De Wolf, D., & Smeers, Y. (2023). Comparison of Battery Electric Vehicles and Fuel Cell Vehicles. *World Electric Vehicle Journal, 14*(9), 262. DOI:10.3390/wevj14090262

Djermouni, K., Berboucha, A., Ghedamsi, K., Aouzellag, D., & Tamalouzt, S. (2024). Energy Management Applied To Non-Autonomous Photovoltaic Station For Hybrid Vehicle Loading. *Journal of Renewable Energies, EEIC'2023 (Special Issue)*, 33-45.

El Ouanjli, N., Derouich, A., El Ghzizal, A., et al. (2019). Modern improvement techniques of direct torque control for induction motor drives - a review. *Protection and Control of Modern Power Systems, 4*, 11. DOI:10.1186/s41601-019-0125-5

Hu, J. S., Yin, D., & Hu, F. R. (2011). A robust traction control for electric vehicles without chassis velocity. In S. Soylu (Ed.), *Electric Vehicles - Modelling and Simulations* (1st ed., pp. 107-126). Croatia. DOI:10.5772/16942

Huang, B., Su, L., & Ren, Y. (2017). DC/DC Converter Common Mode EMI in Parallel-Series PHEV. *Electrotehnica, Electronica, Automatica (EEA), 66*(1), 41-46.

Jasthi, K., & Gampa, S. R. (2023). Direct Torque Control of an Induction Motor Using Fractional-Order Sliding Mode Control Technique for Quick Response and Reduced Torque Ripple. *World Electric Vehicle Journal, 14*(6), 137. DOI:10.3390/wevj14060137

Li, J., Zhu, Y., & Xu, Y. (2014). Research on control strategy optimization in power transmission system of hybrid electric vehicle. *Machinery Design & Manufacture, 67*(3), 138-141.

Liu, Y., Chen, D., & Lei, Z. (2017). Modeling and control of engine starting for a full hybrid electric vehicle based on system dynamic characteristics. *International Journal of Automotive Technology, 18*(5), 911-922. DOI:10.1007/s12239-017-0089-2

Mihăescu, M., & Popescu, D. (2018). Simulink modelling of transient operating regimes of a four-port DC-DC converter used in hybrid vehicles. *Electrotehnica, Electronica, Automatica (EEA), 66*(3), 26-34.

Sayeh, K. F., Tamalouzt, S., Ziane, D., Sahri, Y., Deffaf, B., & Lalouni Belaid, S. (2024). Control of a Wind Turbine based on DFIG by Improved Direct Torque Control using Fuzzy Logic. *Journal of Renewable Energies, EEIC2023 (Special Issue)*, 71-78. DOI:10.54966/jreen.v1i1.1173

Tazerart, F., Mokrani, Z., Rekioua, D., & Rekioua, T. (2015). Direct torque control implementation with losses minimization of induction motor for electric vehicle applications with high operating life of the battery. *International Journal of Hydrogen Energy*, *40*(39), 13827-13838. DOI:10.1016/j.ijhydene.2015.04.052

Tazerart, F., Taïb, N., Rekioua, T., Rekioua, D., & Tounzi, A. (2014). Direct torque control optimization with loss minimization of induction motor. In *Conférence Internationale en Sciences Technologies Electriques au Maghreb-CISTEM, Tunis*. Publisher: IEEE. DOI:10.1109/CISTEM.2014.7077002

Xingzhi, H. (2017). Analysis of Traction Control System in Hybrid Electric Vehicle based on Engine-Motor Coordinated Control Strategy. *Electrotehnica, Electronica, Automatica (EEA), 65*(3), 42-48. DOI:10.3390/wevj5020460

Yue, H., Lin, J., Dong, P., Chen, Z., & Xu, X. (2023). Configurations and Control Strategies of Hybrid Powertrain Systems. *Energies, 16*(2), 725. DOI :10.3390/en16020725

Zhang, N., Zhao, F., & Luo, Y. (2014). A dynamic coordinated control strategy for the mode-switch of HEV based on motor speed closed-loop control. *Automotive Engineering*, *36*(2), 134-138. DOI:10.1007/978-3-642-33777-2_34

Zidane, N., & Lalouni Belaid, S. (2024). Energy management for renewable electricity production system including hybrid hydrogen sub-system. *Journal of Renewable Energies, EEIC2023 (Special Issue)*, 107-115. DOI :10.54966/jreen.v1i1.1198